Bioconjugate Chemistry

Article

pubs.acs.org/bc

Cyclic RGD Peptide Incorporation on Phage Major Coat Proteins for Improved Internalization by HeLa Cells

Dong Shin Choi,[†,§] Hyo-Eon Jin,[†,§] So Young Yoo,[†,§,‡] and Seung-Wuk Lee*[,†,§]

[†]Department of Bioengineering, University of California, Berkeley, California 94720, United States

[§]Physical Bioscience Division, Lawrence Berkeley National Laboratory, Berkeley, California 94720, United States

[‡]Convergence Stem Cell Research Center, Pusan National University School of Medicine, Yangsan 626-870, South Korea

Supporting Information

ABSTRACT: Delivering therapeutic materials or imaging reagents into specific tumor tissues is critically important for development of novel cancer therapeutics and diagnostics. Genetically engineered phages possess promising structural features to develop cancer therapeutic materials. For cancer targeting purposes, we developed a novel engineered phage that expressed cyclic RGD (cRGD) peptides on the pVIII major coat protein using recombinant DNA technology. Using a type 88 phage engineering approach, which inserts a new gene to express additional major coat protein in the noncoding region of the phage genome, we incorporated an additional pVIII major coat protein with relatively bulky cRGD and assembled heterogeneous major coat proteins on the F88.4 phage surfaces. With IPTG control, we could tune different numbers of cRGD peptide displayed on the phage particles up to 140 copies. The resulting phage with cRGD on the recombinant pVIII protein exhibited enhanced internalization efficiency into HeLa cells in a ligand density and conformational structure dependent manner when comparing with the M13 phages modified with either linear RGD on pVIII or cRGD on pIII. Our cRGD peptide engineered phage could be useful for cancer therapy or diagnostic purposes after further modifying the phage with drug molecules or contrast reagents in the future.

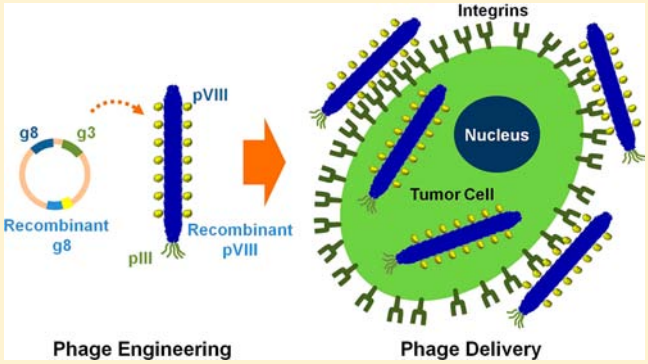

INTRODUCTION

Specific delivery of therapeutic materials or imaging reagents into desired cancerous tissues or organs is critically important for the development of novel therapeutic methods or early diagnosis of cancers.[1−4] Cancer remains a major cause of considerable morbidity and mortality worldwide with approximately one in four deaths in the United States due to the disease.[5] In order to develop nanomedicine for cancer diagnosis and therapy, specifically targeted delivery of therapeutic materials into desired cancer tissues is considered one of the most critical components to enhancing the efficacy of current cancer medicines.[6−8] Many limitations of conventional chemotherapeutics - such as instability in circulation, inadequate tissue distribution, and toxicity to normal cells - could be improved through targeted delivery. Advancements in nanoscale and biological engineering of viral particles provide for the development of novel pathways to develop nanomedicine for cancer therapeutics. Various types of viruses, such as adenovirus, adeno-associate virus, and bacteriophages, have already been utilized for targeted cancer therapy and imaging after genetic and chemical modification.[9−19]

In comparison with other virus-based targeted drug delivery approaches, methods utilizing bacteriophages possess multiple advantages as a targeted drug delivery vehicle: phages can easily be altered by introducing functional peptides for new targeting and therapeutic functions using a recombinant DNA technology;[10,20−23] desired targeting peptide sequences can be identified through a high-throughput evolutionary screening processes (phage display);[24−26] relatively large genes can be introduced without disrupting the phage's own packaging process;[27,28] outer protein shells protect the gene;[9,14,29] and chemical modification can expand the phage's capabilities toward biomedical imaging and the incorporation of anticancer, therapeutic molecules.[23,30,31]

Previously, phage-mediated drug and gene delivery into mammalian cells was developed based on known targeting peptide motifs or newly identified peptide information as determined by phage display.[9,11,14,16,25,29,32−39] The resulting phages functionalized with targeting peptide sequences could deliver therapeutic molecules or genes to specific cancer tissues or organs. The most widely used peptide for targeting cancer is the integrin binding motif (Arg-Gly-Asp; RGD).[3,35,36,38,40−44] Integrins represent a major family of cellular receptors specific to extracellular protein ligands, many of which interact with the RGD sequence on target proteins.[40,41,45] Because integrins are overexpressed in cancerous tissues, research groups have

Received: July 11, 2013
Revised: November 25, 2013
Published: December 15, 2013

dx.doi.org/10.1021/bc4003234 | *Bioconjugate Chem.* 2014, 25, 216−223

utilized the RGD motif to target these tissues in order to study cancer.[3,14,21,35,38] The RGD peptide in different ligands (i.e., fibrinogen, vitronectin, and fibronectin) binds to specific integrins with different affinities dependent upon factors such as conformation and neighboring amino acid sequences.[34,35,41,42,46] Previous studies have shown that cyclic RGD can bind to integrins 10 times stronger than the linear RGD peptide due to its structural stability.[42] Various RGD peptide structures have previously been incorporated on the phage's major and minor coat proteins.[20,35,36,38,42,47]

There are several phage engineering approaches to display functional peptides on their coat proteins (Figure 1A). A type 3 approach has the capability to display five copies of relatively large functional peptides or proteins (up to 50 mer) on the N-terminus of the pIII region so that the phage could express either linear or cyclic RGD peptides on the pIII minor coat protein.[36] A type 8 phage engineering approach would allow us to modify the major coat protein surface with relatively small peptides (up to 8 mer).[48,49] Previously, our research group incorporated the linear RGD peptide onto the M13 phage's pVIII major coat protein and used these engineered phages for fabricating novel tissue engineering materials and gene delivery materials.[21,23,50−55] Although cyclic RGD has enhanced biochemical activity, it is challenging to incorporate a circular motif on the major coat protein, since the pVIII major coat proteins must be closely packed in order to form the phage particles, and such modifications can cause instability of the phage packaging and propagation processes.

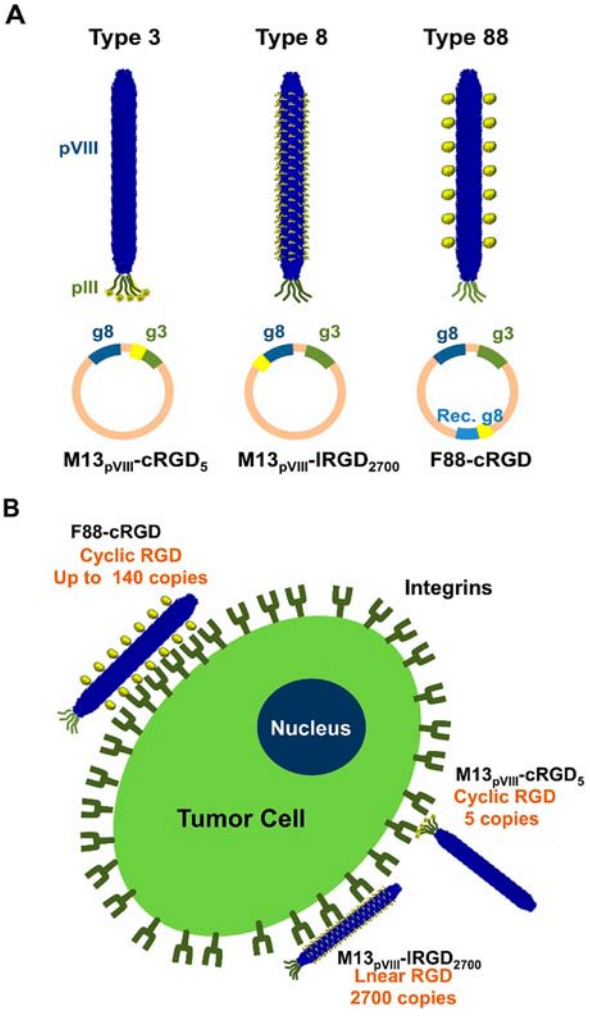

Figure 1. Three different types of phage engineering approaches and targeted delivery to cancer cells. (A) Incorporation of the phage with target peptides using Type 3, Type 8, and Type 88 approaches. Type 3 phage can display five copies of cyclic RGD on the pIII protein. Type 8 phage can display 2700 copies of RGD, but only in linear form. Using Type 88 phage engineering, cyclic RGD can be incorporated in the recombinant pVIII protein up to 140 copies. (B) Schematic illustration of the targeted delivery of the engineered phage to cancer cells.

In order to improve the integrin targeting capability of the phage, we can further engineer the phage major coat proteins using type 88 phage engineering approaches on F88.4 phage (Figure 1A). In the type 88 phage engineering approach, the phage genome has two different genes to encode the pVIII protein: a wild-type g8 and a recombinant g8, respectively. In this system, the wild-type g8 can be utilized to help keep the phage pVIII protein intact, while the recombinant g8 encodes a new major coat protein (recombinant pVIII) fused with a functional peptide/protein. In addition, the recombinant pVIII can accommodate relatively large or structurally bulky inserts that cannot be tolerated by the wild-type pVIII coat proteins.[56] We hypothesized that the cyclic RGD peptide can be incorporated on the phage major coat protein using the type 88 phage engineering approach and the resulting phage will significantly enhance the targeting to and internalization activity of the cancer cells. Here, we developed a phage to express a cyclic RGD peptide (cRGD) on the pVIII major coat protein using the type 88 phage engineering approach. We utilized the F88.4 phage genome to insert additional genes and expressed different numbers of cRGD on the major coat proteins of the phage by controlling isopropyl β-D-1-thiogalactopyranoside (IPTG) levels. We showed that the resulting phage with cRGD on the major coat proteins exhibited enhanced interaction with the target HeLa cell in a ligand density dependent manner. The resulting phage showed the increased internalization efficiency by the HeLa cells when compared to both linear RGD peptides on the major coat and cRGD peptides on minor coat proteins on the control phages. Our engineered phage may have applications in targeted drug or gene delivery for cancer therapeutics or diagnostics in the future.

METHODS AND MATERIALS

Materials and reagents. The Fd-tet and F88.4 phages were kindly provided by Smith group from University of Missouri (University of Missouri, MO). Enzymes utilized for genetic engineering of phage - *Hin*dIII, T4 DNA ligase, and Phusion High-Fidelity DNA polymerase - were purchased from New England Biolabs (Beverly, MA). Oligomers were ordered from Integrated DNA Technologies (Chicago, IL) and Invitrogen (Carlsbad, CA). Isopropyl-β-D-thiogalactopyranoside (IPTG) was purchased from Apex Bioresearch Products (San Diego, CA). QIAprep Spin Miniprep Kit for the extraction of dsDNA from *E. coli* was purchased from Qiagen (Hilden, Germany). HeLa human cervical cancer cells were obtained from the cell facility at the University of California, Berkeley (Berkeley, CA). DMEM media, Trypsin-EDTA solution, fetal bovine serum (FBS), and 1% antibiotics−antimicotics were purchased from Gibco Life Technologies (Carlsbad, CA). The rabbit anti-fd primary antibody was purchased from Sigma Aldrich (St. Louis, MO). Alexa Fluor 594 fluorochrome-conjugated goat anti-rabbit antibody, Alexa Fluor 488

dx.doi.org/10.1021/bc4003234 | Bioconjugate Chem. 2014, 25, 216−223

phalloidin, and DAPI were purchased from Invitrogen (Carlsbad, CA). All other chemicals and solvents used in this study were of analytical or high-performance liquid chromatography (HPLC) grade and purchased from Sigma Aldrich (St. Louis, MO).

Genetic Engineering of F88.4 Phage. The F88.4 phage vector was engineered to display the cyclic RGD (cRGD) peptide motif on recombinant pVIII coat proteins by using the inverse polymerase chain reaction (PCR) cloning method.[21,22,52] Details on the primers used can be found in Table S1. To incorporate the gene sequences, PCR was performed using Phusion High-Fidelity DNA Polymerase, the two primers, and an F88.4 vector. The PCR product was purified using an agarose gel, eluted with spin column purification (Qiagen), digested with *Hin*dIII enzyme, and recircularized overnight at 16 °C with T4 DNA Ligase. The ligated DNA vector was then transformed into XL-10 Gold *E. coli* competent cells (Stratagene, La Jolla, CA), and the amplified plasmid was verified via DNA sequencing at the UC Berkeley DNA Sequencing Facility (Berkeley, CA). The engineered phage was amplified in NZY media (Fisher Scientific, Pittsburgh, PA) by infecting a midlog culture of XL-10 Gold and purified by PEG solution containing 20% (w/v) polyethylene glycol (PEG)-8000 and 2.5 M NaCl as previously described.[21,25,57] While other phage constructs were amplified without IPTG, the engineered F88.4-cRGD phage was amplified with the induction of cRGD peptide by various concentrations of IPTG treatment. To maximize the expression of recombinant cRGD, different IPTG concentrations ranging from 0.3 mM to 5 mM were used when producing the phage. The M13 phage with the cRGD peptide on the pIII minor coat proteins and linear RGD peptide on the pVIII major coat proteins was constructed previously in our laboratory and used in the internalization studies (see Table S2).[21,22,50,52]

Induction and Verification of Recombinant pVIII Peptide on F88.4 Phage. To investigate the expression levels of cyclic RGD on the phage coat protein, SDS-PAGE and MALDI-TOF analysis were utilized. For SDS-PAGE, phage particles were disassembled with 6 M of guanidine-HCl and maintained at 95 °C for 5 min, after which the phage proteins were loaded onto the tricine-SDS-PAGE midi gels (Bio-Rad, Hercules, CA). After electrophoresis, Coomassie staining was performed on the gel. In addition, MALDI-TOF mass spectrometry (Voyager-DE PRO, Applied Biosystems, Carlsbad, CA) was utilized to quantify the amount of recombinant pVIII peptide on the phage surface induced by the various concentrations of IPTG. Bovine insulin from Sigma Aldrich (St. Louis, MO) was utilized as a standard to calibrate the molecular weight. Since the intensity of the MALDI-TOF signal represented the relative amount of the protein in the same batch, we were able to measure the relative amount of specific proteins in a sample.[20,58] In order to disassemble the phage, 1 mg/mL of each type of phage was incubated with 6 M of guanidine-HCl for 5 min. The phage proteins were transferred to the matrix buffer (acetonitrile) using C4 ZipTip (Millipore, Temecula, CA), and loaded on the plate for the MALDI-TOF analysis.

Cell Culture. HeLa cells were cultured in a T-75 flask (Nunc, Rochester, MN) in DMEM media supplemented with 10% FBS and 1% antibiotics–antimicotics at 37 °C, 5% CO_2, and 95% humidity, and the growth media was changed every 2 days. For the phage internalization experiments, HeLa cells were seeded in Lab-TekII Chamber Slide (Thermo-Fisher Scientific, Rochester, NY) at a density of 5×10^4 cells/well and were grown overnight.

Phage Internalization Studies with Different F88-cRGD Phages. F88-cRGD phages amplified with 0.3 mM, 1.5 mM, 3 mM, 5 mM of IPTG were diluted in the HeLa cell culture media to 7.5×10^{10} phage/mL. Triplicate wells with HeLa cells cultured overnight (seeded with the 5×10^4 cells/well) were blocked with 1% normal BSA in the cell culture media for 30 min and treated with 0.2 mL of each phage. The phages were incubated with the HeLa cells for 4 h at 37 °C. The nonbound phages were removed by washing the cells three times with PBS. The wells were then prepared for fluorescent microscopy.

Phage Internalization Studies with Different Phage Types. Three types of engineered phages (i.e., cyclic RGD on recombinant pVIII proteins of F88.4 phage, linear RGD on pVIII major coat protein of M13 phage, and cyclic RGD on pIII minor coat protein of M13 phage) were exposed to HeLa cells for the phage internalization assay. Chamber slides were blocked with 1% normal BSA in the cell culture media for 30 min before phage treatment followed by the addition of 1.5×10^{10} phages/well. The samples were then incubated for 4 h at 37 °C. The nonbound phages were washed away three times with PBS and the wells were prepared for fluorescence microscopy.

Quantification of Internalized Phage by Fluorescent Microscopy Images. The cells were washed with 0.1 M glycine (pH 2.0) containing 1 mg/mL BSA to wash the cell surface bound phage and were then rinsed with PBS. Cells were fixed in 3.7% formaldehyde solution for 15 min at room temperature and washed three times with PBS. Cells were made permeable by incubation with 0.1% Triton X-100 for 15 min and washed with PBS. To detect internalized phages, samples were blocked with 1% normal BSA in PBS for 30 min. Primary antibodies for identifying cell markers and the phage were incubated with the cells for 4 h. The cells were treated with rabbit anti-fd primary antibody (1:500 dilution in PBST) and washed with PBST three times, then incubated with Alexa Fluor 594 fluorochrome-conjugated goat anti-rabbit antibody (1:500 dilution in PBST) and washed three times with PBST. Actin filaments and nuclei were stained with Alexa Fluor 488 phalloidin and DAPI, respectively, as counterstaining for all samples. The fluorescence images were collected using an IX71 Fluorescence Microscope (Olympus, Tokyo, Japan). To quantify the internalized phage from the fluorescence images, we utilized the CellProfiler v 2.0 (Broad Institute, Cambridge, MA) which is an open-source software that can quantitatively measure the amount of the fluorescently labeled material from a series of the images.[59,60]

Statistical Analysis. All results from *in vitro* experiments were expressed as a mean ± SD of three independent experiments. Comparison among multiple groups was performed using one-way ANOVA with the Tukey test. $p < 0.05$ was considered to be the minimal level of significance.

RESULTS AND DISCUSSION

We utilized F88.4 phage to express the cyclic RGD through the type 88 phage engineering approach (Figure 1). The F88.4 phage, which was derived from Fd-tet phage,[25] possesses two g8 genes to encode two pVIII major coat proteins: One is a wild-type gene and the other is an extra recombinant pVIII major coat protein.[25,61] The Fd-tet and F88.4 phages were kindly provided by Smith group from University of Missouri. In

the F88.4 system, an additional gene (recombinant g8) was added to the noncoding part of the phage genome. We added both the signaling peptide and the recombinant pVIII gene to the phage genome and induced the resulting proteins to go through the phage assembly process. While conventional pVIII major coat engineering (type 8 phage engineering) allows for the expression of up to eight additional amino acids on the pVIII major coat proteins,[48,49] type 88 phage engineering allows for the insertion of relatively large bulky peptide inserts on the major coat protein. We constructed the F88.4 phage genome to display the cRGD (termed F88-cRGD) using primers shown in Table S1. The peptide sequence of the cRGD displayed was Cys-Gly-Arg-Gly-Asp-Ser-Cys-Gly-Gly-Gly (Figure S1A). The two cysteines on both ends of the GRGDS peptide help in generation of the cyclic form of RGD by forming a disulfide bond. Three glycines (Gly-Gly-Gly) were added as a flexible linker that helps the cRGD to protrude from the phage surface. The size of the resulting engineered phage genome was analyzed using gel electrophoresis after treatment with a restriction enzyme to linearize the genome (Figure S1B). The gel images showed the proper propagation of the DNA band when compared to the wild-type genome. While the wild F88.4 phage genome has 9183 bps, the F88-cRGD phage has 9254 bps. 328 bps of the noncoding region in the Fd-tet phage genome was replaced with 399 bps of recombinant pVIII that included the gene encoding cRGD.

For the comparison purposes, we engineered phage constructs by expressing the RGD on different coat proteins of M13 phages which have similar protein structures to the Fd-tet phage (see Table S2). Using an M13 phage system, we could engineer the same cyclic CGRGDSC on the pIII protein ($M13_{pVIII}$-$cRGD_5$), while the pVIII proteins only accepted linear GRGDS ($M13_{pVIII}$-$lRGD_{2700}$).[21,52,54] Though we were able to construct phage vectors to encode cyclic RGD sequence using the M13 phage, those phage vectors were not able to produce phage particles. When linear and cyclic forms of RGD are expressed as a fusion protein at the end of the N-terminal of the pVIII major coat protein, those inserts are known to influence their packing stability. The major coat proteins are assembled on the phage with the fivefold helical symmetry through the long axis of the phage.[25,48,49] We believe that the modification of the cyclic structure on the RGD through the Cys-Cys disulfide bond significantly influences packing stability of the phage so that we could not construct the phage with the cyclic RGD. Therefore, we exploited the type 88 approach of the F88.4 phage to incorporate cRGD on the major coat protein. Although M13 and F88.4 phage possess similar filamentous structures, F88.4 has 2012 bps longer genome due to the tetracycline gene and the recombinant gene for the recombinant pVIII expression. Because of the length difference in their genomes, the M13 phage has 2700 copies of pVIII and the F88.4 has 4000 copies of pVIII.[25,61] In our experiment, the cyclic RGD was incorporated to the F88.4 phage so that some portions of 4000 pVIII proteins were substituted with the recombinant pVIII protein as reported previously.[61,62]

The F88-cRGD phage displayed the cRGD in an IPTG concentration dependent manner. The expression of the recombinant pVIII protein is controlled by IPTG by inserting a tac promoter in the front of the recombinant g8, whereas the wild-type gene 8 is transcribed constitutively. The resulting phage particles are covered with a mosaic of wild-type and recombinant pVIII molecules.[61−65] Because expressions of the recombinant major coat proteins are controlled by IPTG, we could control the expressed amount of recombinant pVIII by tuning the IPTG concentration between 0.3 mM and 5 mM. In other words, we could manipulate the ratio of the recombinant pVIII to the wild-type pVIII by changing the IPTG concentration.

The amount of recombinant pVIII on the F88-cRGD phage surface was quantified in two ways: SDS-PAGE (sodium dodecyl sulfate polyacrylamide gel electrophoresis) and MALDI-TOF (matrix-assisted laser desorption ionization time-of-flight) analysis (Figure 2). The phage proteins were

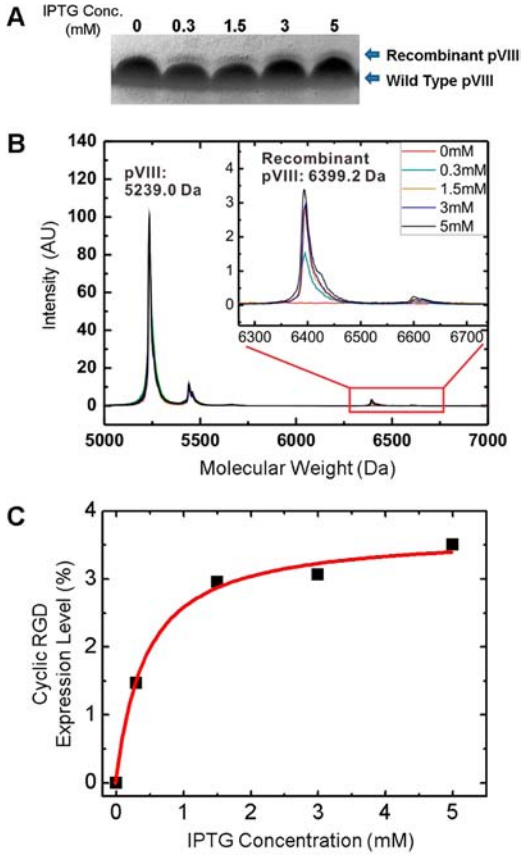

Figure 2. Analyses of the recombinant pVIII protein expression on the phage. (A) Expression levels of recombinant pVIII on the phage via SDS-PAGE using F88-cRGD phages amplified with different IPTG concentrations (0, 0.3, 1.5, 3, and 5 mM of IPTG). (B) MALDI-TOF analyses of recombinant pVIII protein expression on the phage. (C) Percentage of the recombinant pVIII protein when compared to the wild-type version on each phage amplified in different IPTG concentrations (0, 0.3, 1.5, 3, and 5 mM of IPTG). Red line represents the fitting curve.

first denatured and then loaded onto the tricine-SDS-PAGE midi gels (Bio-Rad, Hercules, CA). The expected molecular weight of the wild-type pVIII and the recombinant pVIII is 5239.0 and 6399.2 Da, respectively. For their relatively small amount compared to the pVIII, other phage structural proteins, such as pIII, pVI, pVII, and pIX, are not visible on the gel. While the wild-type Fd-tet phage showed only one band for the wild pVIII protein, the F88-cRGD phages exhibited two bands: a wild-type pVIII and a recombinant pVIII protein (Figure 2A). Because the molecular weights of the two proteins are too close to separate, we could not confirm that the expression level of recombinant pVIII protein increased by the increase of IPTG concentration (Figure 2A).

dx.doi.org/10.1021/bc4003234 | Bioconjugate Chem. 2014, 25, 216−223

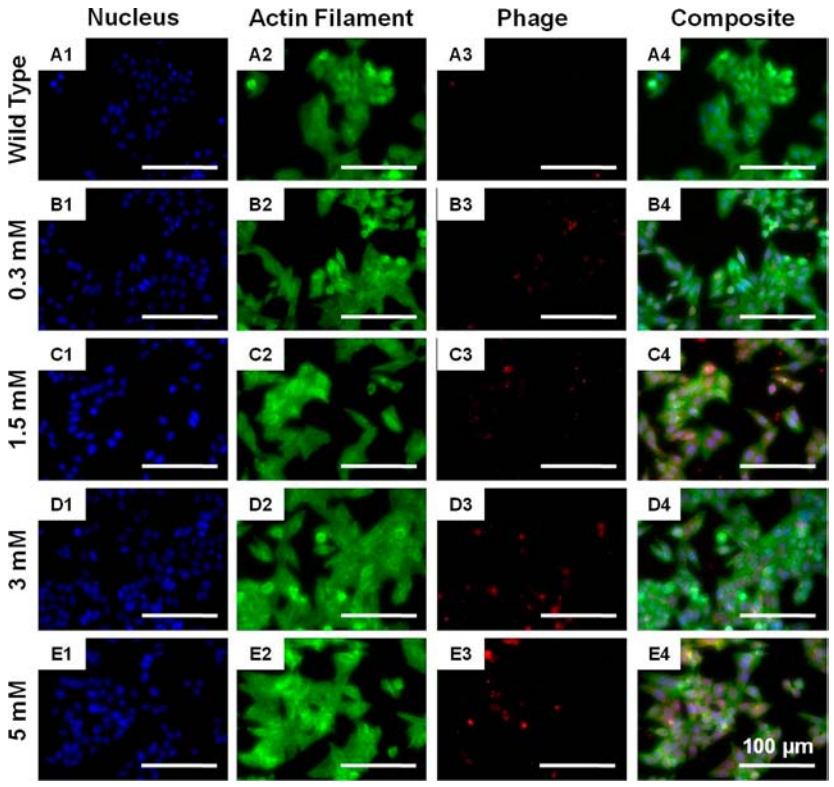

Figure 3. Immunofluorescence images after treatment of the F88-cRGD phages. HeLa cells were incubated with either wild-type F88.4 phage (A) or F88-cRGD phages amplified with different IPTG concentrations: 0.3 mM (B), 1.5 mM (C), 3 mM (D), and 5 mM (E) of IPTG. (1) Blue: DAPI, nucleus; (2) Green: actin filaments; (3) Red: phages; (4) composite images of 1, 2, and 3. Scale bars are 100 μm.

We quantified the relative expression amounts of the recombinant pVIII protein using MALDI-TOF (Figure 2B). For quantification of a certain protein, the protein with a known amount should be set as a control.[66,67] However, in this work, we focused on the relative amount of the recombinant pVIII compared to wild-type pVIII. By setting the original wild-type pVIII amount as the control, we could obtain the relative amount of the recombinant pVIII for each phage and calculate how much recombinant pVIII was expressed on the phage surface. Expected and calculated molecular weights of peaks are presented for the wild-type pVIII and recombinant pVIII on the Table S3. After collecting MALDI-TOF data from the pVIII protein solution, the maximum intensity of the wild-type pVIII protein peak signals was normalized to 100 and the areas of the wild-type pVIII and the recombinant pVIII protein signals were measured and compared. The relative amount of the recombinant pVIII proteins was estimated and plotted using the ratio between the peak areas of the wild-type and recombinant pVIII proteins (Figure 2C). As the IPTG concentration increased, so did the amount of recombinant pVIII proteins with the incorporated cRGD. The expressed ratio of the recombinant pVIII was gradually increased up to 3% at 1.5 mM and saturated at ~3.5% near 5 mM of IPTG concentration. Previously, it has been known that the number of inserted peptides is restricted by the size and conformation of the inserted residue. Larger inserts tend to reduce the number of the recombinant pVIII. Our results coincide with previous results where 0.5−5% of the wild-type pVIII proteins were substituted to the recombinant pVIII.[62,68] Based on the MALDI-TOF measurements we were able to estimate that the maximum number of recombinant pVIII coat proteins in the F88-cRGD phage was 140 copies (the total number of major coat proteins of the F88.4 is 4000).[61]

We characterized the internalization efficiency of the F88-cRGD phages with different amounts of the cRGD ligand using HeLa cells (Figure 3). The HeLa cell is a well-established cancer cell line known to overexpress integrins on the cellular membrane. Because the RGD motif selectively binds to integrins, the cRGD on the phages can target the HeLa cell. We expected that the phages would bind to the integrins on the HeLa cells causing the bound phages to be internalized by receptor-mediated endocytosis.[35,38,39] In order to quantify the internalization efficiency of the engineered phages, we incubated the HeLa cells with the phages with different amounts of cRGD prepared from IPTG controls. After acid washing to remove the phages bound on the HeLa cell membrane, we used immunofluorescence staining to quantify the internalized phages using CellProfiler (www.cellprofiler.org).[59,60] The immunofluorescence images showed that the phages with the higher number of cyclic RGD peptides exhibited better internalization efficiency (Figure 4). We believe that the improved internalization originates from the increased multivalency of the cRGD peptides on the phages that could have led to more efficient targeting into the cell membrane by integrin receptor-mediated endocytosis. This result was consistent with previous reports that the multimerization of the RGD peptide increased binding affinity to the integrin and elicited higher internalization.[44] When we quantified the fluorescence level, the phage amplified with 5 mM of IPTG was internalized 16.7 times more than that of the wild type phage ($p < 0.001$). These results show that the internalization efficiency is dependent upon the variation of ligand number for each phage particle.

dx.doi.org/10.1021/bc4003234 | Bioconjugate Chem. 2014, 25, 216−223

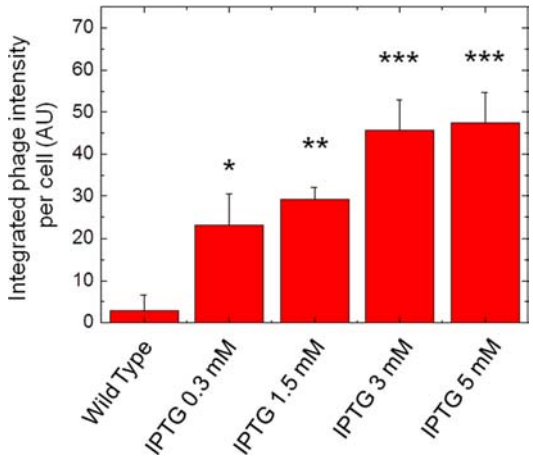

Figure 4. Quantification of the internalized phages with CellProfiler. With enhanced multivalency of the cRGD on the major coat protein of F88.4 phage, more F88-cRGD phages were delivered into HeLa cells due to the increased expression of the cRGD moiety. The F88-cRGD phage amplified with 5 mM of IPTG showed the best internalization efficiency. *p < 0.05; **p < 0.01; ***p < 0.001 from the wild-type phage treated group.

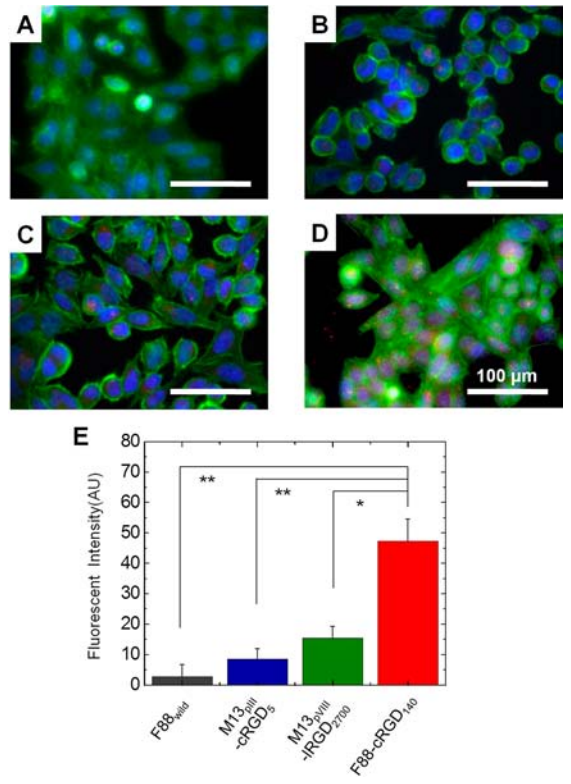

Figure 5. Comparison of different phage engineering strategies for internalization into HeLa cell. HeLa cells were incubated with the different types of engineered phages: (A) F88.4-wild, (B) $M13_{pIII}$-$cRGD_5$, (C) $M13_{pVIII}$-RGD_{2700}, and (D) F88-$cRGD_{140}$ phages for 4 h. Blue: DAPI (nucleus). Green: actin filaments. Red: phages. White scale bars represent 100 μm. (E) Quantification of the internalized of F88-$cRGD_{140}$ phages with the control phages. *p < 0.01, **p < 0.001 from the F88-cRGD phage treated group.

To compare the internalization efficiency of our phage construct with other phages engineered to express the RGD motif, we utilized the M13 phage with cyclic RGD on the pIII protein ($M13_{pIII}$-$cRGD_5$) and linear RGD on the pVIII coat protein ($M13_{pVIII}$-$lRGD_{2700}$) as controls (Figure 1).[21,50,52] Because F88-cRGD phage amplified with 5 mM of IPTG showed the best internalization efficiency, we used the F88-cRGD phage with 5 mM IPTG (termed F88-$cRGD_{140}$) for the comparison experiments. The same number of each type of phage ($F88_{wild}$, $M13_{pIII}$-$cRGD_5$, $M13_{pVIII}$-$lRGD_{2700}$, and F88-$cRGD_{140}$) was incubated with the HeLa cells for 4 h at 37 °C. After acid washing, the immunofluorescence images (Figure 5A–D) were collected and the amounts of internalized phage were calculated via CellProfiler. Among the tested set, the F88-$cRGD_{140}$ phage had the best internalization efficiency (Figure 5E). Because the F88-$cRGD_{140}$ phage carries 140 copies of cRGD on the major coat protein, internalization efficiency of the F88 phage was significantly improved. The F88-$cRGD_{140}$ phage showed 5.5 times better internalization efficiency than that of the $M13_{pIII}$-$cRGD_5$ phage (p < 0.001), and 3.1 times better than the $M13_{pVIII}$-RGD_{2700} phage (Figure 5E, p < 0.01). The $M13_{pIII}$-$cRGD_5$ has 5 copies of the cRGD, while the $M13_{pVIII}$-RGD_{2700} has 2700 copies of linear RGD. The difference of internalization efficiency between type 3 ($M13_{pIII}$-$cRGD_5$) and type 8 ($M13_{pVIII}$-RGD_{2700}) phages is caused by the different numbers of the RGD peptide motif with different specificity caused by the linear or cyclic form of RGD peptides. Even with the linear form of the RGD on the type 8 phage, the excessive amount of RGD on the pVIII major coat protein of the phage induced better interaction with the integrins on the HeLa cells. Though engineering pVIII (type 8 strategies) holds great advantage on the number of ligands, the pVIII is embedded on the surface of the phage particle and linear RGD may not be presented effectively to the integrins.[69] That is one of the critical reasons type 8 (2700 copies of ligand) approaches could not improve the internalization efficiency drastically compared to type 3 (5 copies of ligand) approaches. In our type 88 approach, we could display the cyclic RGD ligand to protrude from the surface of the phage, which could lead to better interaction with the integrins. Although F88-$cRGD_{140}$ phage expressed ∼20 times less RGD peptide than that of the $M13_{pVIII}$-RGD_{2700}, the cyclic form RGD present on the F88-$cRGD_{140}$ phage played a critical role in enhancing the interaction with the HeLa cell and induced integrin-mediated endocytosis.[36,38,39,44] These results showed that type 88 phage engineering is effectively able to display large numbers (∼140 copies) of the functional cyclic form of the RGD peptides on the phage major coat protein.

■ SUMMARY

We genetically engineered a filamentous phage to express the cyclic form of integrin binding peptide, cRGD in the recombinant pVIII major coat protein. We tuned the expression levels of cRGD on the phage surface by the control of IPTG. The resulting phage could express cRGD on the phage surface to make up a maximum of 3.5% of the total number of major coat proteins, corresponding to 140 copies of cRGD. We observed that the internalization efficiency of the cRGD engineered phage into the HeLa cells was increased with the increased copy number of cRGD on the phage. Internalization efficiency of the F88-$cRGD_{140}$ phage, which displayed 140 copies of the cRGD motif, was 5.5 times higher than that of $M13_{pIII}$-$cRGD_5$ phage and 3.1 times higher than $M13_{pVIII}$-RGD_{2700} phage. We believe that the improvement of the internalization efficiency of the phage originated from the stable expression of a large number of copies of the cyclic RGD

dx.doi.org/10.1021/bc4003234 | Bioconjugate Chem. 2014, 25, 216–223

peptides on the pVIII major coat protein through type 88 phage engineering. We believe that our engineered phage could be useful for cancer therapeutics and diagnostics after further modification of the phage proteins with therapeutic materials or contrast reagents.

■ ASSOCIATED CONTENT

Supporting Information

Tables for the sequence of primers and peptides. Table of the molecular weights of wild and recombinant pVIII for different F88-cRGD calculated from MALDI-TOF. Results of phage genome engineering. This material is available free of charge via the Internet at http://pubs.acs.org.

■ AUTHOR INFORMATION

Corresponding Author

*Phone: +1-510-486-4628. Fax: +1-510-486-6488. E-mail: leesw@berkeley.edu.

Author Contributions

Dong Shin Choi and Hyo-Eon Jin contributed equally to this work.

Notes

The authors declare no competing financial interest.

■ ACKNOWLEDGMENTS

We thank Dr. George Smith group for providing F88.4 genome. D.S.C. was supported by the fellowship from Kwanjung Educational Foundation. H.E.J. was supported by Basic Science Research Program through the National Research Foundation of Korea (NRF) funded by the Ministry of Education, Science and Technology (NRF-2011-357-E00083). S.Y.Y. was supported by Basic Science Research Program through the National Research Foundation of Korea (NRF) funded by the Ministry of Science, ICT and Future Planning (2013R1A1A3008484).

■ REFERENCES

(1) Peer, D., Karp, J. M., Hong, S., Farokhzad, O. C., Margalit, R., and Langer, R. (2007) Nanocarriers as an emerging platform for cancer therapy. *Nat. Nanotechnol. 2*, 751−760.

(2) Ferrari, M. (2005) Cancer nanotechnology: opportunities and challenges. *Nat. Rev. Cancer 5*, 161−171.

(3) Desgrosellier, J. S., and Cheresh, D. A. (2010) Integrins in cancer: biological implications and therapeutic opportunities. *Nat. Rev. Cancer 10*, 9−22.

(4) Tennant, D. A., Durán, R. V., and Gottlieb, E. (2010) Targeting metabolic transformation for cancer therapy. *Nat. Rev. Cancer 10*, 267−277.

(5) Siegel, R., Naishadham, D., and Jemal, A. (2013) Cancer statistics, 2013. *CA Cancer J. Clin. 63*, 11−30.

(6) Nie, S., Xing, Y., Kim, G. J., and Simons, J. W. (2007) Nanotechnology applications in cancer. *Annu. Rev. Biomed. Eng. 9*, 257−288.

(7) Brannon-Peppas, L., and Blanchette, J. O. (2004) Nanoparticle and targeted systems for cancer therapy. *Adv. Drug Delivery 56*, 1649−1659.

(8) Zhang, L., Gu, F., Chan, J., Wang, A., Langer, R., and Farokhzad, O. (2007) Nanoparticles in medicine: therapeutic applications and developments. *Clin. Pharmacol. Ther. 83*, 761−769.

(9) Poul, M. A., and Marks, J. D. (1999) Targeted gene delivery to mammalian cells by filamentous bacteriophage. *J. Mol. Biol. 288*, 203−211.

(10) Frenkel, D., and Solomon, B. (2002) Filamentous phage as vector-mediated antibody delivery to the brain. *Proc. Natl. Acad. Sci. U.S.A. 99*, 5675−5679.

(11) Sergeeva, A., Kolonin, M. G., Molldrem, J. J., Pasqualini, R., and Arap, W. (2006) Display technologies: application for the discovery of drug and gene delivery agents. *Adv. Drug Delivery 58*, 1622−1654.

(12) Bedi, D., Gillespie, J. W., Petrenko, V. A., Jr., Ebner, A., Leitner, M., Hinterdorfer, P., and Petrenko, V. A. (2013) Targeted delivery of siRNA into breast cancer cells via phage fusion proteins. *Mol. Pharmacol. 10*, 551−9.

(13) Merzlyak, A., and Lee, S. W. (2006) Phage as templates for hybrid materials and mediators for nanomaterial synthesis. *Curr. Opin. Chem. Biol. 10*, 246−52.

(14) Hajitou, A., Trepel, M., Lilley, C. E., Soghomonyan, S., Alauddin, M. M., Marini, F. C., Restel, B. H., Ozawa, M. G., Moya, C. A., Rangel, R., Sun, Y., Zaoui, K., Schmidt, M., von Kalle, C., Weitzman, M. D., Gelovani, J. G., Pasqualini, R., and Arap, W. (2006) A hybrid vector for ligand-directed tumor targeting and molecular imaging. *Cell 125*, 385−398.

(15) Kota, J., Chivukula, R. R., O'Donnell, K. A., Wentzel, E. A., Montgomery, C. L., Hwang, H.-W., Chang, T.-C., Vivekanandan, P., Torbenson, M., and Clark, K. R. (2009) Therapeutic microRNA delivery suppresses tumorigenesis in a murine liver cancer model. *Cell 137*, 1005−1017.

(16) Müller, O. J., Kaul, F., Weitzman, M. D., Pasqualini, R., Arap, W., Kleinschmidt, J. A., and Trepel, M. (2003) Random peptide libraries displayed on adeno-associated virus to select for targeted gene therapy vectors. *Nat. Biotechnol. 21*, 1040−1046.

(17) Maheshri, N., Koerber, J. T., Kaspar, B. K., and Schaffer, D. V. (2006) Directed evolution of adeno-associated virus yields enhanced gene delivery vectors. *Nat. Biotechnol. 24*, 198−204.

(18) Hedley, S., der Maur, A. A., Hohn, S., Escher, D., Barberis, A., Glasgow, J., Douglas, J., Korokhov, N., and Curiel, D. (2005) An adenovirus vector with a chimeric fiber incorporating stabilized single chain antibody achieves targeted gene delivery. *Gene Ther. 13*, 88−94.

(19) Nishimoto, T., Yoshida, K., Miura, Y., Kobayashi, A., Hara, H., Ohnami, S., Kurisu, K., Yoshida, T., and Aoki, K. (2009) Oncolytic virus therapy for pancreatic cancer using the adenovirus library displaying random peptides on the fiber knob. *Gene Ther. 16*, 669−680.

(20) AndrewáLee, L. (2008) Oriented cell growth on self-assembled bacteriophage M13 thin films. *Chem. Commun.*, 5185−5187.

(21) Yoo, S. Y., Chung, W. J., Kim, T. H., Le, M., and Lee, S. W. (2011) Facile patterning of genetically engineered M13 bacteriophage for directional growth of human fibroblast cells. *Soft Matter 7*, 363−368.

(22) Yoo, S. Y., Kobayashi, M., Lee, P. P., and Lee, S.-W. (2011) Early osteogenic differentiation of mouse preosteoblasts induced by collagen-derived DGEA-peptide on nanofibrous phage tissue matrices. *Biomacromolecules 12*, 987−996.

(23) Bhattarai, S. R., Yoo, S. Y., Lee, S. W., and Dean, D. (2012) Engineered phage-based therapeutic materials inhibit Chlamydia trachomatis intracellular infection. *Biomaterials 33*, 5166−5174.

(24) Winter, G., Griffiths, A. D., Hawkins, R. E., and Hoogenboom, H. R. (1994) Making antibodies by phage display technology. *Annu. Rev. Immunol. 12*, 433−455.

(25) Smith, G. P., and Petrenko, V. A. (1997) Phage Display. *Chem. Rev. 97*, 391−410.

(26) Hoogenboom, H. R. (2005) Selecting and screening recombinant antibody libraries. *Nat. Biotechnol. 23*, 1105−1116.

(27) Seow, Y., and Wood, M. J. (2009) Biological gene delivery vehicles: beyond viral vectors. *Mol. Ther. 17*, 767−777.

(28) Greenstein, D., and Brent, R. (2001) Introduction to vectors derived from filamentous phages. *Curr. Protoc. Mol. Biol.*, 1.14.1−1.14.5..

(29) Hajitou, A., Rangel, R., Trepel, M., Soghomonyan, S., Gelovani, J. G., Alauddin, M. M., Pasqualini, R., and Arap, W. (2007) Design and construction of targeted AAVP vectors for mammalian cell transduction. *Nat. Protoc. 2*, 523−531.

(30) Bar, H., Yacoby, I., and Benhar, I. (2008) Killing cancer cells by targeted drug-carrying phage nanomedicines. *BMC Biotechnol. 8*, 37.

(31) Li, K., Chen, Y., Li, S., Nguyen, H. G., Niu, Z., You, S., Mello, C. M., Lu, X., and Wang, Q. (2010) Chemical modification of M13 bacteriophage and its application in cancer cell imaging. *Bioconjugate Chem. 21*, 1369−1377.
(32) Larocca, D., Jensen-Pergakes, K., Burg, M. A., and Baird, A. (2001) Receptor-targeted gene delivery using multivalent phagemid particles. *Mol. Ther. 3*, 476−484.
(33) Urbanelli, L., Ronchini, C., Fontana, L., Menard, S., Orlandi, R., and Monaci, P. (2001) Targeted gene transduction of mammalian cells expressing the HER2/neu receptor by filamentous phage. *J. Mol. Biol. 313*, 965−976.
(34) Arap, W., Pasqualini, R., and Ruoslahti, E. (1998) Cancer treatment by targeted drug delivery to tumor vasculature in a mouse model. *Science 279*, 377−380.
(35) Koivunen, E., Restel, B. H., Rajotte, D., Lahdenranta, J., Hagedorn, M., Arap, W., and Pasqualini, R. (1999) Integrin-binding peptides derived from phage display libraries, *Integrin Protocols* (Howlett, A., Ed.) pp 3−17, Humana Press, Totowa, NJ.
(36) Koivunen, E., Wang, B., and Ruoslahti, E. (1995) Phage libraries displaying cyclic peptides with different ring sizes: ligand specificities of the RGD-directed integrins. *Biotechnology 13*, 265−70.
(37) Pasqualini, R., and Ruoslahti, E. (1996) Organ targeting in vivo using phage display peptide libraries. *Nature 380*, 364−366.
(38) Pasqualini, R., Koivunen, E., and Ruoslahti, E. (1997) αv integrins as receptors for tumor targeting by circulating ligands. *Nat. Biotechnol. 15*, 542−546.
(39) Ivanenkov, V. V., Felici, F., and Menon, A. G. (1999) Uptake and intracellular fate of phage display vectors in mammalian cells. *BBA-Mol. Cell. Res. 1448*, 450−462.
(40) Ruoslahti, E. (1991) Integrins. *J. Clin. Invest. 87*, 1−5.
(41) Hynes, R. O. (1992) Integrins - versatility, modulation, and signaling in cell-adhesion. *Cell 69*, 11−25.
(42) Koivunen, E., Gay, D. A., and Ruoslahti, E. (1993) Selection of peptides binding to the alpha 5 beta 1 integrin from phage display library. *J. Biol. Chem. 268*, 20205−20210.
(43) Guo, W., and Giancotti, F. G. (2004) Integrin signalling during tumour progression. *Nat. Rev. Mol. Cell Biol. 5*, 816−826.
(44) Jin, Z.-H., Furukawa, T., Waki, A., Akaji, K., Coll, J.-L., Saga, T., and Fujibayashi, Y. (2010) Effect of multimerization of a linear Arg-Gly-Asp peptide on integrin binding affinity and specificity. *Biol. Pharm. Bull. 33*, 370−378.
(45) Humphries, M. J. (1990) The molecular-basis and specificity of integrin ligand interactions. *J. Cell Sci. 97*, 585−592.
(46) Plow, E. F., Dsouza, S. E., and Ginsberg, M. H. (1992) Ligand binding to GPIIb-IIIa: a status report. *Semin. Thromb. Hemost. 18*, 324−332.
(47) Koivunen, E., Wang, B., and Ruoslahti, E. (1994) Isolation of a highly specific ligand for the alpha 5 beta 1 integrin from a phage display library. *J. Cell Biol. 124*, 373−380.
(48) Iannolo, G., Minenkova, O., Petruzzelli, R., and Cesareni, G. (1995) Modifying filamentous phage capsid: limits in the size of the major capsid protein. *J. Mol. Biol. 248*, 835−844.
(49) Makowski, L. (1993) Structural constraints on the display of foreign peptides on filamentous bacteriophages. *Gene 128*, 5−11.
(50) Merzlyak, A., Indrakanti, S., and Lee, S.-W. (2009) Genetically engineered nanofiber-like viruses for tissue regenerating materials. *Nano Lett. 9*, 846−852.
(51) Merzlyak, A., and Lee, S.-W. (2009) Engineering phage materials with desired peptide display: Rational design sustained through natural selection. *Bioconjugate Chem. 20*, 2300−2310.
(52) Yoo, S. Y., Merzlyak, A., and Lee, S.-W. (2011) Facile growth factor immobilization platform based on engineered phage matrices. *Soft Matter 7*, 1660−1666.
(53) Chung, W.-J., Oh, J.-W., Kwak, K., Lee, B. Y., Meyer, J., Wang, E., Hexemer, A., and Lee, S.-W. (2011) Biomimetic self-templating supramolecular structures. *Nature 478*, 364−368.
(54) Chung, W.-J., Merzlyak, A., and Lee, S.-W. (2010) Fabrication of engineered M13 bacteriophages into liquid crystalline films and fibers for directional growth and encapsulation of fibroblasts. *Soft Matter 6*, 4454−4459.
(55) Yoo, S. Y., Choi, D. S., Kobayashi, M., Farouz, Y., Wang, S., and Lee, S.-W. (2013) M13 and AAV Hybrid Phage Tissue Matrices For Topical Gene Delivery.
(56) Smith, G. P., and Fernandez, A. M. (2004) Effect of DNA copy number on genetic stability of phage-displayed peptides. *Biotechniques 36*, 610−618.
(57) Kehoe, J. W., and Kay, B. K. (2005) Filamentous phage display in the new millennium. *Chem. Rev. 105*, 4056−4072.
(58) Swatkoski, S., Russell, S., Edwards, N., and Fenselau, C. (2007) Analysis of a model virus using residue-specific chemical cleavage and MALDI-TOF mass spectrometry. *Anal. Chem. 79*, 654−658.
(59) Carpenter, A. E., Jones, T. R., Lamprecht, M. R., Clarke, C., Kang, I. H., Friman, O., Guertin, D. A., Chang, J. H., Lindquist, R. A., and Moffat, J. (2006) CellProfiler: image analysis software for identifying and quantifying cell phenotypes. *Genome Biol. 7*, R100.
(60) Lamprecht, M. R., Sabatini, D. M., and Carpenter, A. E. (2007) CellProfiler: free, versatile software for automated biological image analysis. *Biotechniques 42*, 71−75.
(61) Enshell-Seijffers, D., Smelyanski, L., and Gershoni, J. M. (2001) The rational design of a 'type 88' genetically stable peptide display vector in the filamentous bacteriophage fd. *Nucleic Acids Res. 29*, e50.
(62) Zwick, M. B., Shen, J., and Scott, J. K. (2000) Homodimeric peptides displayed by the major coat protein of filamentous phage. *J. Mol. Biol. 300*, 307−320.
(63) Zhong, G. (1998) Conformational Mimicry Through Random Constraints Plus Affinity Selection, *Combinatorial Peptide Library Protocols* pp 165−173, Springer.
(64) Malik, P., Terry, T. D., Gowda, L. R., Langara, A., Petukhov, S. A., Symmons, M. F., Welsh, L. C., Marvin, D. A., and Perham, R. N. (1996) Role of capsid structure and membrane protein processing in determining the size and copy number of peptides displayed on the major coat protein of filamentous bacteriophage. *J. Mol. Biol. 260*, 9−21.
(65) Greenwood, J., Willis, A. E., and Perham, R. N. (1991) Multiple display of foreign peptides on a filamentous bacteriophage: peptides from Plasmodium falciparum circumsporozoite protein as antigens. *J. Mol. Biol. 220*, 821−827.
(66) Domon, B., and Aebersold, R. (2006) Mass spectrometry and protein analysis. *Science 312*, 212−217.
(67) Szájli, E., Fehér, T., and Medzihradszky, K. F. (2008) Investigating the quantitative nature of MALDI-TOF MS. *Mol. Cell. Proteomics 7*, 2410−2418.
(68) Perham, R. N., Terry, T. D., Willis, A. E., Greenwood, J., Marzo Veronese, F., and Appella, E. (1995) Engineering a peptide epitope display system on filamentous bacteriophage. *FEMS Microbiol. Rev. 17*, 25−31.
(69) Sidhu, S. S. (2001) Engineering M13 for phage display. *Biomol. Eng. 18*, 57−63.